# Hybrid Polymer–Silicon Proton Conducting Membranes via a Pore-Filling Surface-Initiated Polymerization Approach

**Basit Yameen,[†] Anke Kaltbeitzel,[†] Gunnar Glasser,[†] Andreas Langner,[‡] Frank Müller,[‡] Ulrich Gösele,[‡] Wolfgang Knoll,[§] and Omar Azzaroni*[,||]**

Max-Planck-Institut für Polymerforschung, Ackermannweg 10, 55128 Mainz, Germany, Max-Planck-Institut für Mikrostrukturphysik, Weinberg 2, 06120 Halle, Germany, Austrian Institute of Technology, Donau-City-Strasse 1, 1220 Vienna, Austria, and Instituto de Investigaciones Fisicoquímicas Teóricas y Aplicadas (INIFTA), Universidad Nacional de La Plata, CONICET, CC 16 Suc. 4 (1900), La Plata, Argentina

**ABSTRACT** An alternative approach for the creation of proton conducting platforms is presented. The methodology is based on the so-called "pore-filling concept", which relies on the filling of porous matrices with polyelectrolytes to obtain proton conducting platforms with high dimensional stability. Polymer–silicon composite membranes, with well-defined polyelectrolyte microdomains oriented normal to the plane of the membrane, were prepared using photoelectrochemically etched silicon as a microstructured scaffold. Ordered two-dimensional macroporous silicon structures were rendered proton conducting by filling the micropores via a surface-initiated atom transfer radical polymerization process. The morphological aspects, chemical stability, and performance of the hybrid assemblies were characterized by a set of techniques including scanning electron microscopy, Fourier transform infrared spectroscopy, X-ray photoelectron spectroscopy, nuclear magnetic resonance and impedance spectroscopy, among others. The fabricated silicon-poly(sodium 2-acrylamide-2-methylpropane sulfonate) hybrid membranes displayed proton conductivities in the range of $1 \times 10^{-2}$ S/cm. This work illustrates the potential of hybrid polymer–silicon composite membranes synthesized by pore-filling surface-initiated polymerization to create proton conducting platforms in a simple and straightforward manner. Versatility and relative ease of preparation are two key aspects that make this approach an attractive alternative for the molecular design and preparation of proton conducting systems.

**KEYWORDS:** thin films • polymer brushes • nanotechnology • proton transport • materials science • fuel cells

## INTRODUCTION

During the past decade increasing attention has been focused on finding new avenues to produce proton exchange membranes (PEMs). The reason for this ever-growing interest lies in the fact that PEMs are key constituting elements, with strong implications on the performance of many technological devices, as is the case of future power sources for automotive, stationary, and portable applications. Typical examples of their technological applications include fuel cell vehicles, mobile devices, or power stations for home use (1–4).

As a general rule, PEMs must display good proton conductivity and exhibit good chemical resistance and mechanical strength. Perfluorinated polyelectrolytes like Nafion or Flemion have been used for this purpose for a long time. In fact, in the case of Nafion, it has been historically considered as "the golden standard" (5–8). However, these perfluorinated polymers display several deficiencies, as they are costly to produce and lack mechanical strength and dimensional stability. These polymers consist of a hydrophobic fluorocarbon backbone and hydrophilic sulfonic pendant chains that produce a microphase-separated morphology in the membrane architecture, thus leading to the creation of hydrophilic channels for the proton transport (4). Regarding this latter, we have to note that recent work by Buratto and co-workers demonstrated by using conductive atomic force microscopy that 60% of the hydrophilic domains at the surface of an operating Nafion membrane remain inactive (9).

All these drawbacks with regards to the use of perfluorinated polyelectrolytes acted as a driving force for the development of alternative approaches to PEMs. In recent years, the scientific community actively explored a wide variety of strategies ranging from the use of phosphoric acid-based membranes to layer-by-layer polyelectrolyte films (10–29). Another interesting class of ionically conductive polymers comprises aromatic polymers functionalized with sulfonic acid groups. Sulfonated polyaromatics are commonly prepared either by post sulfonating an existing polymer or by reacting sulfonated monomers in condensation reactions (30). In many cases, depending on sulfonation level, the postsulfonation strategy is preferable (31) because it requires only one reaction step and can be carried out using commercially available, cost-effective starting materi-

* To whom correspondence should be addressed. E-mail: azzaroni@inifta.unlp.edu.ar. Web site: http://softmatter.quimica.unlp.edu.ar.
Received for review October 10, 2009 and accepted December 11, 2009
[†] Max-Planck-Institut für Polymerforschung.
[‡] Max-Planck-Institut für Mikrostrukturphysik.
[§] Austrian Institute of Technology.
[||] Universidad Nacional de La Plata.
DOI: 10.1021/am900690x

als. In contrast, many of the monomers used in the condensation polymerization strategy are not commercially available and require multistep synthesis. Within this framework, poly(2-acrylamide-2-methylpropane sulfonic acid) (polyAMPS), a polyelectrolyte bearing sulfonic acid groups ($-SO_3H$), has been prepared and employed in electrochromic devices as proton conductor. Interestingly, the conductivity of poly-AMPS was found to be comparable with that of Nafion under the same water content (15 $H_2O$ per sulfonic acid group) (32−34). Okada and co-workers have also reported that complex membranes using polyAMPS and polyvinyl alcohol (PVA) displayed proton conductivities comparable with Nafion 117 (35−37). In line with these results, a number of new polymers based on the copolymerization of AMPS monomer with other monomers have been synthesized in recent years (38).

On the other hand, the fabrication of porous scaffolds containing highly ordered and monodispersed nanochannels is also attracting increasing interest as an alternative route to manipulate proton conduction (39). Recently, Yang and co-workers demonstrated the use of aligned mesoporous silica as powerful platforms to modulate the proton transport across thin films acting as membranes (40). Rather than relying on the phase segregation of the perfluorinated polymers, the new emerging approaches are based on generating the channels with robust and durable scaffolds and then incorporating into them the proton conducting source. Within this framework, we should mention the "pore-filling concept" (41−43). This methodology is based on impregnating and filling porous substrates with proton conducting polymers, thus resulting in the creation of matrices with proton conductive properties and excellent mechanical properties. In this context, filling the pores of track-etched membranes with polyelectrolytes resulted in a new class of composite membrane in which the filling material enabled the fine-tuning of the transport characteristics and the track-etched membrane itself provided the required mechanical stability and durability (44−49). These results prompted further investigation into the use of polyelectrolytes confined within pores as platforms for channeling the transport of species (50−58). However, one important drawback of this powerful approach concerns on the stability of the polyelectrolyte confined in the pore. In most cases, the polyelectrolyte was physically adsorbed or impregnated within the porous membrane. This implies that the polyelectrolyte filling is intrinsically unstable in humid environments, leading to the leaching of the filling material. In this regards, some research efforts were recently devoted to overcome this serious limitation. Elabd and co-workers described the use of commercial polycarbonate track-etched (PCTE) membranes as host matrices filled with PolyAMPS via plasma-induced surface graft polymerization (59, 60). In this case, the plasma polymerization process provided robust linkages between the polyelectrolyte and polycarbonate matrix (61), thus increasing the durability of the composite and eliminating potential leaching of the polyelectrolyte under hydrated conditions.

In this work, we describe a different approach to fabricate composite proton conducting membranes based on the surface-initiated polymerization of poly-AMPS from photoelectrochemically etched silicon membranes. The chemical nature of the silicon scaffold enables the use of a very robust anchoring chemistry, as the silane linkage is, to immobilize the polymerization initiators. Then, surface-initiated atom transfer radical polymerization provided the route to the facile synthesis of dense polyelectrolyte layers covaletly tethered to the pore wall (62−67). These results describing the use of highly ordered macroporous silicon modified with polyelectrolyte brushes allowed for the generation of artificial proton conducting channels with conductivity values in the $1 \times 10^{-2}$ S/cm range. We believe that this approach constitutes a valuable alternative for the preparation of robust proton conducting systems with potential applications on the large-scale fabrication of membranes suitable for different industrial applications.

## EXPERIMENTAL SECTION

**Materials and Methods.** Sodium 2-acrylamino-2-methylpropane sulfonate was obtained from ABCR GmbH & Co. KG, Karlsruhe, Germany. (3-Aminopropyl)triethoxysilane 99%, 2-bromopropionyl bromide 97%, 2,2′-bipyridine 99%, and copper(II) chloride, $CuCl_2$, ≥98% (Fluka), were used as-received from Sigma-Aldrich, Schnelldorf, Germany. Sodium chloride 99.99% was obtained from Merck, Darmstadt, Germany. Triethylamine was refluxed overnight with calcium hydride before distilling and stored under argon. Dry dichloromethane was obtained from Acros organics, Geel, Belgium. $^1$H NMR was performed on a Bruker Spectrospin 250 MHz NMR spectrometer (Fallanden, Switzerland). Scanning Electron Microscopy (SEM) was performed with a LEO Gemini 1530 SEM. Atomic absorption spectroscopy (AAS) was performed on a Perkin-Elmer 5100 ZL spectrometer working in flame emission mode. The proton conductivity was measured by dielectric spectroscopy using either an Alpha high-resolution dielectric analyzer equipped with a Novocontrol active sample cell to expand the frequency range to ∼10 MHz or an SI 1260 impedance/gain-phase analyzer. XPS measurements were carried out using a Physical Electronics 5600A instrument. The Mg Kα (1253.6 eV) X-ray source was operated at 300 W. The XPS scans were analyzed using the MultiPak 5.0 software.

**Synthesis of Initiator (1) for SI-ATRP.** Two grams of (3-aminopropyl)triethoxysilane and 1.13 g of triethylamine in 40 mL of dry dichloromethane were mixed, stirred, and gradually cooled to 0 °C. A 50% by volume solution of 2.56 g of 2-bromopropionyl bromide in dry dichloromethane was dropped in the reaction mixture over a period of 30 min and the reaction mixture was allowed to stir at 0 °C for 6 h under $N_2$(g). The reaction mixture was then filtered to remove the $Et_3N^+Br^-$ salt precipitated during the reaction and residue was washed with small amount of dichloromethane. The filtrate was washed with brine (3 × 25 mL). The organic phase was dried over $MgSO_4$ and the solvent was removed in vacuo to yield 2-bromo-2-methyl-*N*-(3-triethoxysilyl-propyl)-propionamide **1** as a colorless oil-like liquid (yield = 66%). $^1$H NMR (250 MHz, CDCl3): $\delta$ 6.8 (1H, *s*), 3.76 (6H, *q*, $J = 6.9$), 3.21 (2H, *q*, $J = 6.6$ Hz), 1.88 (6H, *s*), 1.57 (2H, *m*), 1.16 (9H, *t*, $J = 6.9$), 0.58 (2H, *t*, $J = 8$ Hz).

**Anchoring 1 onto the Surface of Macroporous Silica and Subsequent PEB Growth by SI-ATRP.** The plasma-activated macroporous silica membranes were placed in a Schlenk tube containing 5 μL of **1** in 10 mL of dry toluene at 120 °C for 6 h under $N_2$(g). The membranes were then subjected to ultrasonication for 5 min in each of toluene, ethanol, and THF. After

drying with a stream of $N_2$(g), the membranes were stored under $N_2$(g) until further use. Thick sulfonate PEB was grown on macroporous silica functionalized with **1**. The polymerization procedure is as follows:

Three grams of the sodium 2-acrylamino-2-methylpropane sulfonate was dissolved by stirring in 5.2 mL of 2:1 methanol/water solvent mixture at room temperature. To this solution 0.12 g of BiPy and 2.1 mg of Cu(II)$Cl_2$ were added. The mixture was stirred and degassed by $N_2$(g) bubbling for an hour before 31 mg of Cu(I)Cl was added. The mixture was degassed with $N_2$(g) bubbling for another 15 min. Initiator-coated macroporous silica samples were sealed in a Schlenk tube and degassed by four high vacuum pump/$N_2$(g) refill cycles. The reaction mixture was syringed into this Schlenk tube, adding enough to cover the sample completely, and the mixture was left overnight under $N_2$(g). The samples were removed and thoroughly rinsed with deionized water. After the polymerization, the macroporous silica with PEB was extensively rinsed with water and kept overnight in 0.01N aq. HCl for exchanging the $Na^+$ ions that originally coordinated the monomer with $H^+$.

**Stability Evaluation of PolyAMPS under Acidic Conditions.** PolyAMPS was dissolved in 0.1N HCl aq. solution. The solution was left to stir at room temperature for 1 week followed by 1 week of dialysis (MWCO = 3500). The dialyzed solution was lyophilized to give a white polymer. $^1$H NMR spectra prior to and after the acid treatment were used to observe the hydrolysis.

**Fabrication of the Macroporous Silicon Scaffolds.** The samples were fabricated using a lithographic prestructuring process (68−70). Briefly, in the first step, the initiation spots for the pores were defined photoligraphically on the (100)-oriented n-type silicon wafer. Subsequent alkaline etching formed etch pits that served as pore nuclei. The macropores were obtained by applying a photoelectrochemical etching process. To enable electrochemical dissolution of n-type silicon in HF, electronic holes had to be generated by light absorption. For this purpose, the sample was inserted in an etch cell with its front side exposed to aqueous HF while the back was illuminated. The sample was anodically biased via a transparent back side ohmic contact and the cathode was formed by a platinum wire immersed in HF solution. The photogenerated holes diffused from the wafer back side to the etch front and were consumed by the etch process at the pore tips. This promoted dissolution of the silicon almost exclusively at the pore tips leading to further pore growth perpendicular to the Si(100) surface. Electrochemically etched macroporous silicon exhibited pores with a diameter in the micrometer regime and a depth of up to the thickness of the silicon wafer.

**Effective Loading by Weighing the Macroporous Silica Membrane after Each Step of Functionalization.** A 36.82 mg piece of the initiator-modified porous silicon membrane weighed 38.49 mg after growing the PEB by SI-ATRP followed by extensive washing with water, exchange of $K^+$ counterions with $H^+$, drying with a stream of $N_2$, and overnight storage under a vacuum at room temperature. The mass change reflected a 4.3% increase in weight during the functionalization of the membrane with the polyelectrolyte brush.

**Ion Exchange Capacity.** A 38.49 mg piece of porous silicon−PEB hybrid membrane in $-SO_3H$ form was immersed in 15 mL of 2 mM solution of NaCl. After 24 h the concentration of $Na^+$ in the supernatant was reduced to 1.64 mM as determined by AAS. The ion exchange capacity of the membrane was calculated from eq 1 and was found to be 0.14 meq/g of the porous silica−PEB hybrid membrane.

$$\mathrm{IEC} = \left(\frac{M_1 - M_2}{W}\right)V \qquad (1)$$

$M_1$ and $M_2$ are the molarities of the NaCl solution before and after immersing the porous silica−PEB hybrid membrane, $W$ is the weight of the membrane, and $V$ is the volume of the NaCl solution in which the porous silica−PEB hybrid membrane were immersed.

**Water Uptake Study.** Water uptake was measured gravimetrically. The porous silicon−-PEB hybrid membrane was weighed after exposing to 100% relative humidity (RH) for 24 h ($W_h$). Subsequently, the membrane was allowed to dry first under ambient atmosphere (31% RH) followed by evacuating at 50 °C for 2 h and weighed ($W_{dry}$). The water uptake ($WU$) of 7% (±1%) was calculated from eq 2

$$WU = \left(\frac{W_h - W_{dry}}{W_h}\right)100 \qquad (2)$$

**Proton Conductivity Measurements.** The proton conductivity was measured by dielectric spectroscopy in a two-electrode geometry. The combination of high conductivity and thin sample can lead to distortions of impedance plots above 1 MHz. We have initially used an Alpha high-resolution dielectric analyzer and a Novocontrol active sample cell to expand the frequency range to ~10 MHz. After proving that the resonance is below 1 MHz, wee recorded the spectra using an SI 1260 impedance/gain-phase analyzer and a Novocontrol broadband dielectric converter. An atmosphere of saturated humidity was generated by using a closed sample cell with a water reservoir at the bottom that was not in contact with the sample. Saturation was controlled by a Sensirion SHT75 humidity sensor and found to be 100%, within the error bar of the sensor (2%). Humidity between 18 and 95% was created using a temperature controlled climate chamber (Binder KBF 240). From the Cole−Cole and Bode plots, the resistance of the composite membrane was estimated, and then the specific conductivity of the composite membrane was calculated using the apparent thickness and electrode area.

## RESULTS AND DISCUSSION

**Surface-Initiated Atom Transfer Radical Polymerization of Poly(sodium 2-acrylamide-2-methylpropane sulfonate) Brushes on Planar Surfaces.** During the past decade atom transfer radical polymerization (ATRP) emerged as a most versatile synthetic tool to grow a plethora of monomer units, including charged ones (71−76). This led to the widespread use of ATRP to synthesize different polyelectrolyte architectures. Despite this fact, the use of ATRP to grow poly(sodium 2-acrylamide-2-methylpropane sulfonate) has been less frequently studied than sulfonated polyelectrolytes bearing other chemical functionalities (77, 78). First, in order to corroborate if surface-initiated atom transfer radical polymerization of poly(sodium 2-acrylamide-2-methylpropane sulfonate) brushes is feasible, we studied the brush growth from planar surfaces. We used 2-bromo-2-methyl-*N*-(3-triethoxysilyl-propyl)-propionamide self-assembled monolayers as surface-confined ATRP initiator (Figure 1).

Synthesis of polyelectrolyte brushes bearing sulfonate moieties was carried out using aqueous ATRP of the AMPS monomer, in the sodium salt form, following previously reported procedures (79). Briefly, the polymerization solution consisted of the Cu(I)/ Bipy catalyst (promoting the activation), Cu(II)/Bipy deactivator (promoting capping), and

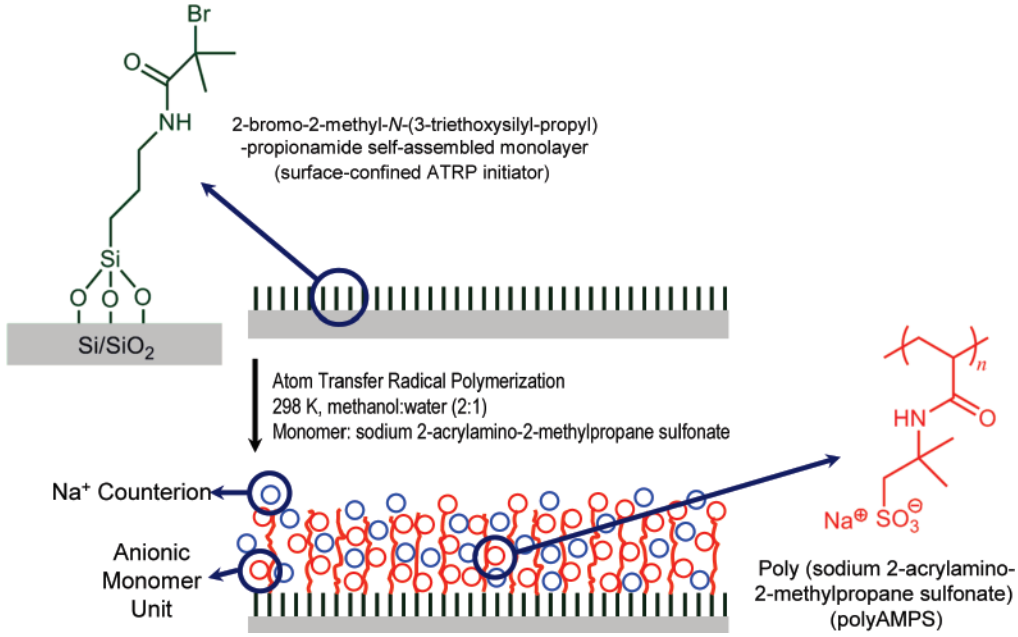


**FIGURE 1. Synthesis of poly(sodium 2-acrylamide-2-methylpropane sulfonate) (polyAMPS) brushes using surface-initiated atom transfer radical polymerization (ATRP).**

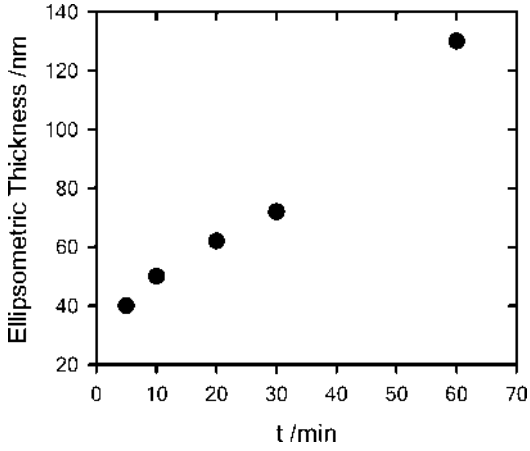


**FIGURE 2. Time-resolved growth of poly(sodium 2-acrylamide-2-methylpropane sulfonate) brushes on silicon surfaces by surface-initiated atom transfer radical polymerization. The polymerization used a monomer concentration of 2.5 M in a methanol/water (2:1) solvent mixture at room temperature. The errors bars are smaller than the symbol size.**

the monomer (AMPS, sodium salt) in an aqueous methanolic solvent. The ratio between Cu(I) and Cu(II) thus determines the rate of polymerization and if, e.g., the Cu(I) concentration is increased, the reaction rate will increase as well. The aqueous environment leads to strongly accelerated polymerization, leading to full conversion in minutes instead of hours or days (80). The substrates are left in the polymerization solution for a certain period of time and then copiously rinsed with water to yield smooth, covalently attached poly(sodium 2-acrylamide-2-methylpropane sulfonate) brushes of varying thicknesses according to the polymerization time (Figure 2). Under our experimental conditions (see Experimental Section for details), 50 min of surface-initiated polymerization led to the formation of 100 nm thick brushes (the average growth rate was 1.6 nm/min). It is worthwhile indicating that for surface-initiated atom transfer radical polymerization (ATRP), a constant radical concentration should yield a linear relationship between film thickness and polymerization time if mass transfer of monomers to the growing radicals is constant. However, although ATRP is often a controlled/living process, it is well-known that the growth rate of polymer films during surface-initiated ATRP frequently decreases with time. The data displayed in Figure 2 describe a fairly rapid brush growth (~8 nm/min) during the early stages of polymerization (<5 min) followed by a moderate decline for longer polymerization times. This observation suggests that termination (presumably because of radical coupling), loss of active catalyst, or hindered mass transport of monomers to radicals may be limiting, at some extent, the surface-initiated polymerization process.

The chemical composition of the synthesized brushes was then corroborated by FTIR and spectroscopy (Figure 3), which revealed the presence of the main chemical groups corresponding to the polyAMPS.

Considering that the anionic polymer brushes are planned to be used as proton sources, we proceeded to study the stability of the brushes in highly acidic environments during the exchange of sodium ions by protons. XPS analysis confirmed that $Na^+$ counterions were effectively removed from the sulfonated brush film during overnight treatment with 0.1 N HCl (Figure 4).

FTIR spectroscopy also indicated that no appreciable degradation of the brush film is observed after immersing the substrates in 0.1 N HCl during one week. In a similar vein, comparative XPS analysis of the surface surface atomic concentrations performed on $Na^+$-coordinated and protonated polyAMPS brushes (Table 1) revealed that the ion exchange procedure in aqueous HCl did not hydrolyze the brushes, i.e., no evidence of quantitative changes in chemical composition were detected.

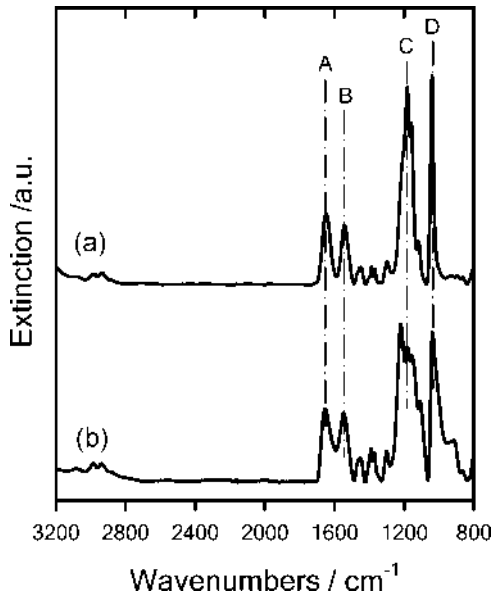


FIGURE 3. FTIR corresponding to polyAMPS brushes (a) prior to and (b) after proton exchange of $Na^+$ in 0.1 N HCl. The indicated IR signals are: (A) 1650 $cm^{-1}$ (C═O) vibration mode, (B) 1564 $cm^{-1}$ (N−H) bending mode, (C) 1182 $cm^{-1}$ asymmetric sulfonate stretching, (D) 1037 $cm^{-1}$ symmetric sulfonate stretching.

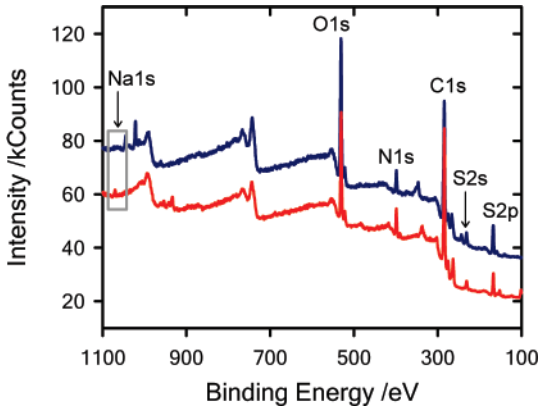


FIGURE 4. Survey XP spectra of polyAMPS brushes prior to (red trace) and after (blue trace) proton exchange of $Na^+$ counterions in 0.1 N HCl. The area delimited by the gray frame highlights the disappearance of the tenuous signal corresponding to the Na 1s photoelectrons after ion exchange

**Table 1. Surface Atomic Concentrations of Protonated and $Na^+$-Coordinated PolyAMPS Brushes, As Determined by X-ray Photoelectron Spectroscopy (XPS)**

| brush | C (%) | N (%) | O (%) | S (%) | Na (%) |
|---|---|---|---|---|---|
| polyAMPS-Na | 62 | 7 | 23 | 5 | 3 |
| polyAMPS-protonated | 61 | 6 | 27 | 6 | |

In addition, complementary $^1H$ NMR experiments performed in ATRP-grown polyAMPS in solution further corroborated that the polyelectrolyte does not evidence hydrolysis, even after long periods in highly acidic aqueous solutions (Figure 5).

**Growth of Polyelectrolyte Brushes on a Scaffold.** Once corroborated that the formation of protonated polyAMPS brushes is feasible we proceeded to the growth of the hydrophilic proton conducting channels

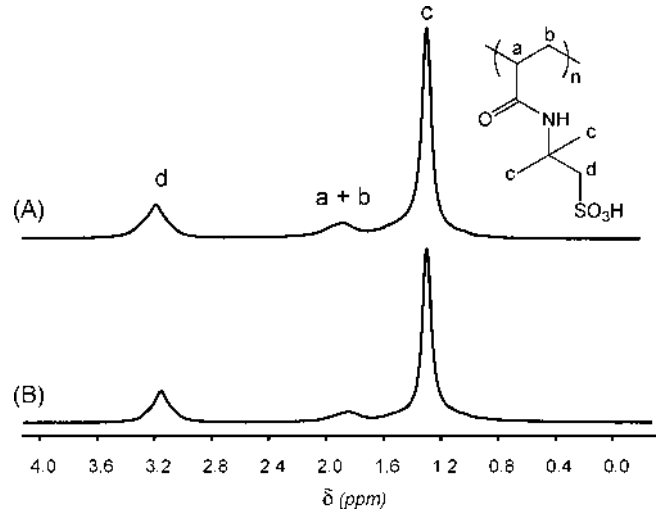


FIGURE 5. Assigned $^1H$ NMR spectra for poly(sodium 2-acrylamide-2-methylpropane sulfonate) before (A) and after (B) stirring during one week in 0.1 N HCl at room temperature. After the acidic treatment, the samples were dialyzed (against pure water) and lyophilized to obtain a solid white polymer.

(Figure 6). The robust scaffold was constituted of photoelectrochemically etched macroporous silicon whose etched area (~3 $cm^2$) was conformed by perfectly parallel channels with a density of ~1 × $10^7$ pores/$cm^2$ (Figure 7).

These macroporous silicon substrates were surface-functionalized with initiator-terminated self-assembled monolayers prior to proceeding with the surface-initiated atom transfer radical polymerization. The polymerization was carried out for overnight followed by careful rinsing with water. Afterward they were placed during 15−20 h in 0.1 N aqueous HCl in order to exchange the $Na^+$ counterions by protons.

Scanning electron microscopy (SEM) imaging revealed that the surface-initiated polymerization led to the homogeneous modification of the silicon membrane resulting in a covalently linked polymer layer evenly distributed on the porous substrate (Figure 8). To further corroborate the success of the SI-ATRP inside the channels, we performed repeated longitudinal cross-sectional analysis of the brush-modified macroporous samples.

Figure 9 clearly indicates that the channels are completely filled with the polyAMPS brushes, thus indicating that the SI-ATRP proceeded smoothly even in the confined environment of the macroporous silicon leading to the formation of robustly "scaffolded" and covalently anchored polyelectrolyte "microrods" (Figure 10) acting as oriented hydrophilic channels and suitable for conducting protons across the silicon membrane.

Once confirmed the successful filling of the micropores with the polyAMPS brushes the proton conductivity of the hybrid membrane was measured using impedance spectroscopy. Results indicated that in humidity saturated atmospheres the membrane displays conductivity values in the range of 1 × $10^{-2}$ S/cm (Figure 11), which is close to the typical values obtained with phase-segregated perfluorinated polyelectrolytes, like Nafion or Flemion (5, 6).

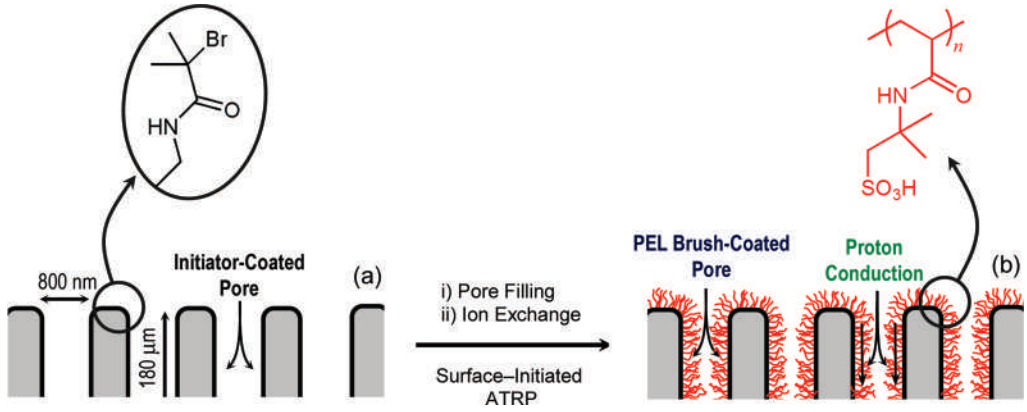


**FIGURE 6. Simplified scheme illustrating the construction of the polyAMPS brush-coated channels. The macroporous silicon membrane modified with 2-bromo-2-methyl-*N*-(3-triethoxysilyl-propyl)-propionamide self-assembled monolayers (a) is immersed in the monomer AMPS-containing ATRP solution where the surface-initiated polyelectrolyte growth is carried out (b).**

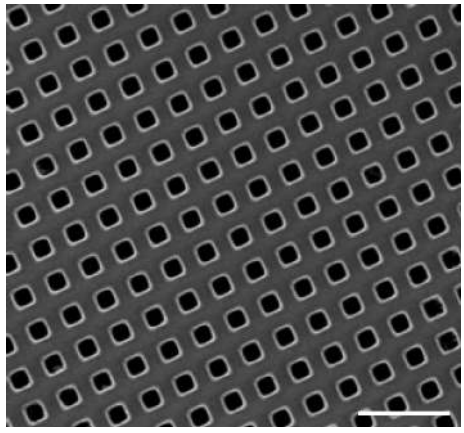

**FIGURE 7. Scanning electron micrograph of the ordered macroporous silicon membrane used as a scaffold for creating the polyelectrolyte-based proton conducting channels. Scale bar: 4.5 $\mu$m. Imaging conditions: landing voltage = 3 KeV@WD = 3 mm; in-lens detector.**

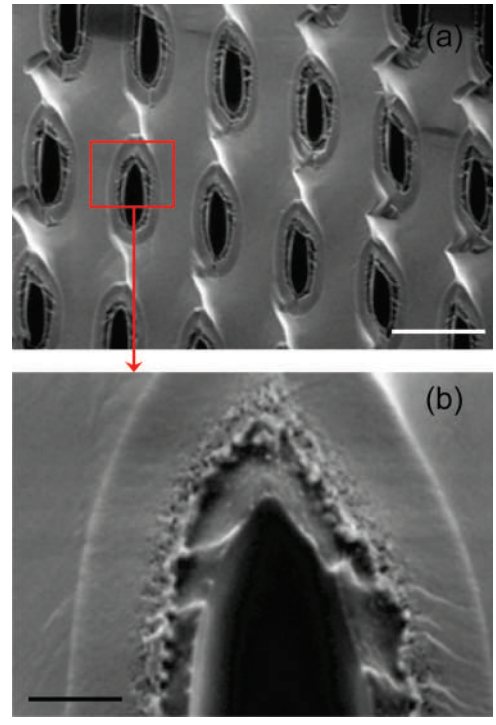


**FIGURE 8. Scanning electron micrographs corresponding to the cross-sectional imaging of a polyAMPS brush-modified silicon membrane at different magnifications: (a) scale bar, 3 $\mu$m; (b) scale bar, 400 nm. Imaging conditions: landing voltage = 0.7 KeV@WD = 1 mm; in-lens detector.**

This can be attributed to the fact that the continuous hydrophilic channels constructed in the membrane facilitate the proton transfer (81−83). This is accomplished in a scenario where part of the protons combined with water molecules generating $H_3O^+$ clusters are transferred through the water channels in the membrane. In addition, part of the protons can be transferred via ionic and hydrogen bonds by jumping from one function to another. It is also worthwhile to mention that the very high density of $-SO_3H$ groups in the brush further shorten the distance between hopping sites, thus leading to a efficient proton conducting pathway. Furthermore, Figure 11 is also evidence that, in close resemblance to Nafion, decreasing the RH promotes a gradual decrease in proton conductivity (84, 85). In the case of phase-segregated perfluorinated polyelectrolytes, the hydrophobic part plays a structural role and acts a scaffold for the immobilization of the sulfonic acid groups ($-SO_3H$) that constitutes the hydrophilic region (where the transport of water and protons occurs). The hydrated morphology of these two-phase systems has a strong impact on the transport of protons in the membrane, whereas a low humidity environment leads to the dehydration and the collapse of the membrane physical architecture. In our case, even though the physical characteristics of the microchannels are not affected by decreasing RH, it is obvious that the dehydration at low RH seriously affects the formation of hydrophilic water channels along the confined polyelectrolyte "microrods".

This approach provides a robust and highly reproducible strategy to firmly anchoring the PEL layer into the channels. This is a major improvement with respect to other methods based on polyelectrolyte impregnation into porous substrates in which humid environments can promote the leakage of the proton conducting polymer. In our case, the chemical nature of the silane linkage provides a robust anchoring for the polyelectrolyte chains which in turn determines the stability of the macromolecular assembly. In addition, it is worth mentioning that this procedure to achieve highly proton conducting membranes is based on

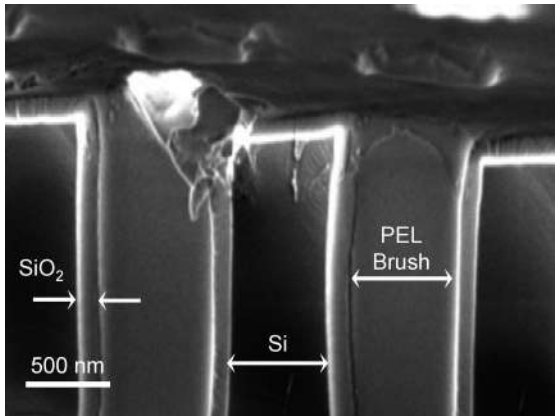


FIGURE 9. Longitudinal cross-sectional SEM imaging of a hybrid polyAMPS brush-silicon membrane. The image shows in detail the filling of the pore as a result of the surface-initiated polymerization. In the figure are also indicated the different constituents of the hybrid membrane. Imaging conditions: landing voltage = 0.7 KeV@WD = 1 mm; in-lens detector.

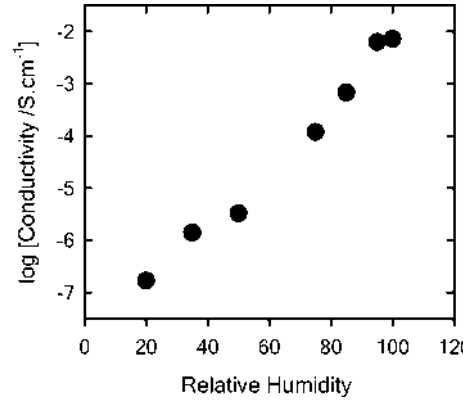


FIGURE 11. Variation of the proton conductivity with increase in relative humidty. Measurements were performed at room temperature. The error bars are smaller than the symbol size.

simple synthetic tools, thus avoiding the use of tedious synthetic routes to achieve proton conducting nanochannels, as is the case of bulk copolymer-based PEMs.

## CONCLUSIONS

The experimental results described in this work illustrate the use of highly ordered macroporous silicon modified with polyelectrolyte brushes as a promising alternative approach to create and molecularly design hybrid conducting membranes. The proposed methodology based on the "pore-filling concept" points to a new direction in the rational design and development of proton conducting platforms. Contrary to what happens in proton-conducting channels generated from microphase-separated block copolymers architectures, this approach introduces a simple strategy to create highly conducting membranes, as demonstrated by proton conductivity values of $\sim 1 \times 10^{-2}$ S/cm, in which the physical architecture is not affected by environmental variables. The use of ATRP to grow the polymers provides a simple and reliable synthetic framework in which a large number of monomers are compatible with the technique, without requiring very demanding reaction conditions. The simple experimental protocols and the large variety of monomers available constitute a toolbox of chemical techniques to be harnessed by chemists, materials scientists, and engineers devoted to the study of proton conducting membranes.

Finally, considering the wide diversity of macroporous silicon architectures that can be fabricated by photoelectrochemical etching, we believe that this approach will serve

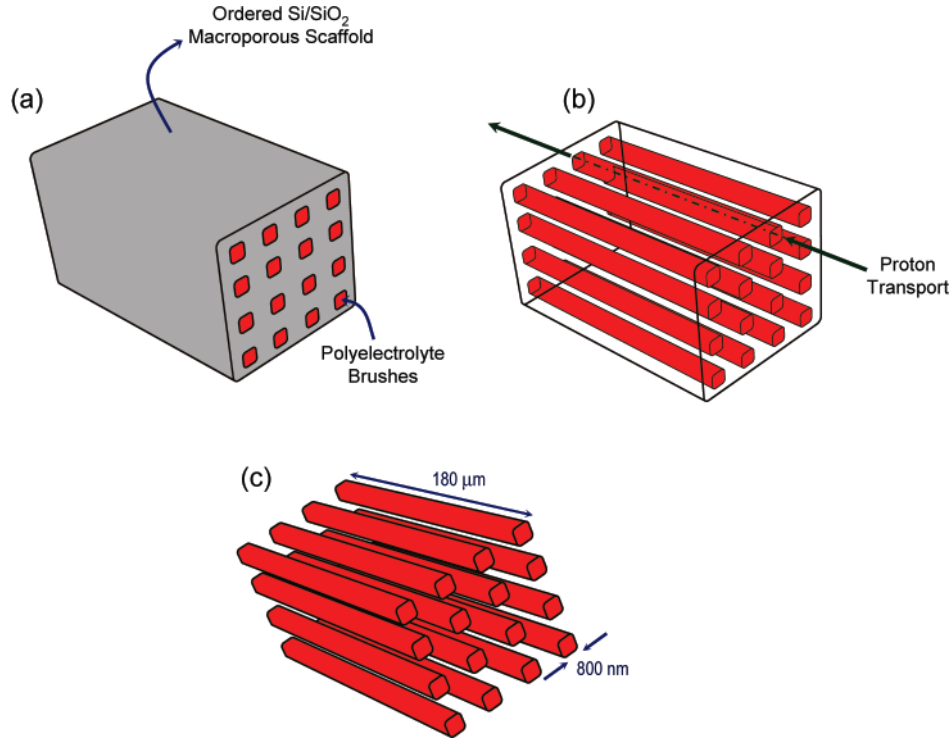


FIGURE 10. Simplified cartoons illustrating: (a) the cross-sectional view of the hybrid membrane, (b) the orientation of the hydrophilic channels/microrods passing through the membrane, and (c) the overall dimensions of the polyelectrolyte brush-based hydrophilic channels.

to the study of model proton conducting systems and could lead, in the not too distant future, to alternative methods for large-scale production PEMs. We envision that much of this success will depend on the synthesis of new monomer units fully compatible with the harsh conditions of fuel-cell operation. As such, we are confident that this approach will turn out to be a proper guidance for further rational molecular design of hybrid proton conducting membranes.

**Acknowledgment.** B.Y. acknowledges financial support from the Higher Education Commission (HEC) of Pakistan and Deutscher Akademischer Austauschdienst (DAAD) (Code #A/04/30795). O.A. is a CONICET fellow and acknowledges financial support from the Max Planck Society (Germany), the Alexander von Humboldt Stiftung (Germany) and the Centro Interdisciplinario de Nanociencia y Nanotecnología (CINN) (ANPCyT, Argentina). We thank Dr. B. Mathias (University of Mainz, Germany) and Daniela Mössner (IMTEK, University of Freiburg, Germany) for AAS and XPS analysis, respectively.

## REFERENCES AND NOTES

(1) Barbir, F. *PEM Fuel Cells: Theory and Practice*; Academic Press: New York, 2005; Chapter 10, pp 337−398.
(2) Srinivasan, S. *Fuel Cells: From Fundamentals to Applications*; Springer: Heidelberg, Germany, 2006; Chapter 10, pp 575−605.
(3) Jacobson, M. Z.; Colella, W. G.; Golden, D. M. *Science* **2005**, *308*, 1901–1905.
(4) Steele, B. C. H.; Heinzel, A. *Nature* **2001**, *414*, 345–352.
(5) Kreuer, K. D. *J. Membr. Sci.* **2001**, *185*, 29–39.
(6) Kreuer, K. D.; Paddison, S. J.; Spohr, E.; Schuster, M. *Chem. Rev.* **2004**, *184*, 4637–4678.
(7) Diat, O.; Gebel, G. *Nat. Mater.* **2008**, *7*, 13.
(8) Schimidt-Rohr, K.; Chen, Q. *Nat. Mater.* **2008**, *7*, 75.
(9) Bussian, D. A.; O'Dea, J. R.; Metiu, H.; Buratto, S. K. *Nano Lett.* **2007**, *7*, 227.
(10) Daiko, Y.; Katagiri, K.; Matsuda, A. *Chem. Mater.* **2008**, *20*, 6405–6409.
(11) Argun, A. A.; Ashcraft, J. A.; Hammond, P. T. *Adv. Mater.* **2008**, *20*, 1539–1543.
(12) Liu, S.; Pu, Q.; Gao, L.; Korzeniewski, C.; Matzke, C. *Nano Lett.* **2005**, *5*, 1389–1393.
(13) Kidena, K. *J. Membr. Sci.* **2008**, *323*, 201–206.
(14) Pereira, F.; Vallé, K.; Belleville, P.; Morin, A.; Lambert, S.; Sanchez, C. *Chem. Mater.* **2008**, *20*, 1710–1718.
(15) DeLongchamp, D. M.; Hammond, P. T. *Langmuir* **2004**, *20*, 5403–5411.
(16) Neburchilov, V.; Martin, J.; Wang, H.; Zhang, J. *J. Power Sources* **2007**, *129*, 221–238.
(17) Honma, I.; Yamada, M. *Bull. Chem. Soc. Jpn.* **2007**, *80*, 2110–2123.
(18) Haile, S. M.; Boysen, D. A.; Chisholm, C. R. I.; Merle, R. B. *Nature* **2001**, *410*, 910–913.
(19) Wainright, J. S.; Wang, J. T.; Weng, D.; Savinell, R. F.; Litt, M. *J. Electrochem. Soc.* **1995**, *142*, L121–L123.
(20) Kannan, R.; Kakade, B. A.; Pillai, V. K. *Angew. Chem., Int. Ed.* **2008**, *47*, 1–5.
(21) Farhat, T. R.; Hammond, P. T. *Adv. Funct. Mater.* **2005**, *15*, 945–954.
(22) Mauritz, K. A.; Moore, R. B. *Chem. Rev.* **2004**, *104*, 4535–4585.
(23) Fang, Y.; Leddy, J. *J. Phys. Chem.* **1995**, *99*, 6064–6073.
(24) Tsang, E. M. W.; Zhang, Z.; Shi, Z.; Soboleva, T.; Holdcroft, S. *J. Am. Chem. Soc.* **2007**, *129*, 15106–15107.
(25) Farhat, T. R.; Hammond, P. T. *Adv. Funct. Mater.* **2006**, *16*, 433–444.
(26) Hartmann-Thompson, C.; Merrington, A.; Carver, P. I.; Keeley, D. L.; Rousseau, J. L.; Hucul, D.; Bruza, K. J.; Thomas, L. S.; Keinath, S. E.; Nowak, R. M.; Katona, D. M.; Santurri, P. R. *J. Appl. Polym. Sci.* **2008**, *110*, 959–974.
(27) DeLongchamp, D. M.; Hammond, P. T. *Langmuir* **2004**, *20*, 5403–5411.
(28) DeLongchamp, D. M.; Hammond, P. T. *Chem. Mater.* **2003**, *15*, 1165–1173.
(29) Lutkenhaus, J. L.; Hammond, P. T. *Soft Matter* **2007**, *3*, 804–816.
(30) Hickner, M. A.; Ghassemi, H.; Kim, Y. S.; Einsla, B. R.; McGrath, J. E. *Chem. Rev.* **2004**, *104*, 4587–4612.
(31) Iojoiu, C.; Marechal, M.; Chabert, F.; Sánchez, Y. J. *Fuel Cells* **2005**, *5*, 344.
(32) Harris, C. S.; Rukavina, T. G. *Electrochim. Acta* **1995**, *40*, 2315–2320.
(33) Huang, Y. H.; Chen, L. C.; Ho, K. C. *Solid State Ionics* **2003**, *165*, 269–277.
(34) Randin, J. P. *J. Electrochem. Soc.* **1982**, *129*, 1215–1220.
(35) Qiao, J.; Ikesaka, S.; Saito, M.; Kuwano, J.; Okada, T. *Electrochem. Commun.* **2007**, *9*, 1945–1950.
(36) Qiao, J.; Hamaya, T.; Okada, T. *Polymer* **2005**, *46*, 1−808–10816.
(37) Manaya, T.; Inoue, S.; Qiao, J.; Okada, T. *J. Power Sources* **2006**, *156*, 311–324.
(38) Paneva, D.; Mespouille, L.; Manolova, L.; Degée, P; Rashkov, I.; Dubois, P. *Macromol. Rapid Commun.* **2006**, *27*, 1489–1494.
(39) Ding, J.; Chuy, C.; Holdcroft, S. *Chem. Mater.* **2001**, *13*, 2231–2233.
(40) Fan, R.; Huh, S.; Yan, R.; Arnold, J.; Yang, P. *Nat. Mater.* **2008**, *7*, 303.
(41) Yamaguchi, T.; Miyazaki, Y.; Nakao, S.-i.; Tsuru, T.; Kimura, S. *Ind. Eng. Chem. Res.* **1998**, *37*, 177–184.
(42) Yamaguchi, T.; Nakao, S.-I.; Kimura, S. *J. Polym. Sci., Part B: Polym. Phys.* **1997**, *35*, 469–477.
(43) Mika, A. M.; Childs, R. F.; Dickson, J. M.; McCarry, B. E.; Gagnon, D. R. *J. Membr. Sci.* **1995**, *108*, 37–56.
(44) Nishimura, H.; Yamaguchi, T. *Electrochem. Solid-State Lett.* **2004**, *7*, A385–A388.
(45) Yildirim, M. H.; Schwarz, A.; Stamatalis, D. F.; Wessling, M. *J. Membr. Sci.* **2009**, *328*, 127–133.
(46) Kai, T.; Goto, H.; Shimizu, Y.; Yamaguchi, T.; Nakao, S.-i.; Kimura, S. *J. Membr. Sci.* **2005**, *265*, 101–107.
(47) Munakata, H.; Yamamoto, D.; Kanamura, K. *Chem. Comm.* **2005**, 3986–3988.
(48) Yamaguchi, T.; Miyata, F.; Nakao, S.-I. *Adv. Mater.* **2003**, *15*, 1198–1201.
(49) Mika, A. M.; Childs, R. F. *Ind. Eng. Chem. Res.* **2003**, *42*, 3111–3117.
(50) Yamaguchi, T; Kuroki, H.; Miyata, F. *Electrochem. Commun.* **2005**, *7*, 730–734.
(51) Yamaguchi, T.; Zhou, H.; Nakazawa, S.; Hara, N. *Adv. Mater.* **2007**, *19*, 592–596.
(52) Vorrey, S.; Teeters, D. *Electrochim. Acta* **2003**, *48*, 2137–2141.
(53) Dauginet, L.; Duwez, A.-S.; Legras, R.; Demoustier-Champagne, S. *Langmuir* **2001**, *17*, 3852–3857.
(54) Castriota, M.; Teeters, D. *Ionics* **2005**, *11*, 220–225.
(55) Layson, A. R.; Teeters, D. *Solid State Ionics* **2004**, *17*, 773–780.
(56) Li, X. M.; Shen, Z.; He, T.; Wessling, M. *J. Polym. Sci., Part B: Polym. Phys.* **2008**, *46*, 1589–1593.
(57) Zhou, J.; Childs, R. F.; Mika, A. M. *J. Membr. Sci.* **2005**, *254*, 89–99.
(58) Suryanarayan, S.; Mika, A. M.; Childs, R. F. *J. Membr. Sci.* **2007**, *290*, 196–206.
(59) Chen, H.; Palmese, G. R.; Elabd, Y *A Chem. Mater.* **2006**, *18*, 4875–4881.
(60) Chen, H.; Palmese, G. R.; Elabd, Y *A Macromolecules.* **2007**, *40*, 781–782.
(61) Wan, L.-S.; Liu, Z.-M.; Xu, Z.-K. *Soft Matter* **2009**, *5*, 1775–1785.
(62) Calvo, A.; Yameen, B.; Williams, F. J.; Soler-Illia, G. J. A. A.; Azzaroni, O. *J. Am. Chem. Soc.* **2009**, *131*, 10866–10868.
(63) Yameen, B.; Ali, M.; Neumann, R.; Ensinger, W.; Knoll, W.; Azzaroni, O. *Nano Lett.* **2009**, *9*, 2788–2793.
(64) Yameen, B.; Ali, M.; Neumann, R.; Ensinger, W.; Knoll, W.; Azzaroni, O. *Small* **2009**, *5*, 1287–1291.
(65) Yameen, B.; Kaltbeitzel, A.; Langner, A.; Müller, F.; Gösele, U.; Knoll, W.; Azzaroni, O. *Angew. Chem., Int. Ed.* **2009**, *48*, 3124–3228.
(66) Yameen, B.; Ali, M.; Neumann, R.; Ensinger, W.; Knoll, W.; Azzaroni, O. *J. Am. Chem. Soc.* **2009**, *131*, 2070–2071.
(67) Yameen, B.; Kaltbeitzel, A.; Langner, A.; Duran, H.; Müller, F.; Gösele, U.; Azzaroni, O.; Knoll, W. *J. Am. Chem. Soc.* **2008**, *130*, 13140–13144.
(68) Schilling, J.; Müller, F.; Matthias, S.; Wehrspohn, R. B.; Gösele, U.; Busch, K. *Appl. Phys. Lett.* **2001**, *78*, 1180–1182.

(69) Müller, F.; Biner, A.; Gösele, U.; Lehmann, V.; Ottow, S.; Föll, H. *J. Porous Mater.* **2000**, *7*, 201–204.
(70) Ottow, S.; Lehmann, V.; Föll, H. *Appl. Phys. A: Mater. Sci. Process.* **1996**, *63*, 153–159.
(71) Klep, V.; Zdyrko, B.; Liu, Y.; Luzinov, I. In *Polymer Brushes: Synthesis, Characterization, Applications*; Advicnula, R. C., Brittain, W. J., Caster, K. C., Rühe, J., Eds.; Wiley-VCH: Weinheim, Germany, 2004; Chapter 3, pp 69−86.
(72) Granville, A. M.; Boyes, S. G.; Akgun, B.; Foster, M. D.; Constable, A.; Brittain, W. J. In *Responsive Polymer Materials: Design and Applications*; Minko, S., Ed.; Blackwell Publishing: Ames, IA, 2006; Chapter. 4, pp 69−83.
(73) Pietrasik, J.; Bombalski, L.; Cusick, B.; Huang, J.; Pyun, J.; Kowalewski, T.; Matyjaszewski, K. In *Stimuli-Responsive Polymeric Films and Coatings*l Urban, M., Ed.; American Chemical Society: Washington, D.C., 2005; Chapter 2, pp 28−42.
(74) Azzaroni, O.; Moya, S.; Farhan, T.; Brown, A. A.; Huck, W. T. S. *Macromolecules* **2005**, *38*, 10192–10199.
(75) Farhan, T.; Azzaroni, O.; Huck, W. T. S. *Soft Matter* **2005**, *1*, 66–68.
(76) Azzaroni, O.; Brown, A. A.; Huck, W. T. S. *Angew. Chem., Int. Ed.* **2006**, *45*, 1770–1774.
(77) Ramstedt, M.; Cheng, N.; Azzaroni, O.; Mossialos, D.; Mathieu, H. J.; Huck, W. T. S. *Langmuir* **2007**, *23*, 3314–3321.
(78) Calvo, A.; Yameen, B.; Williams, F. J.; Azzaroni, O.; Soler-Illia, G. J. A. A. *Chem. Commun.* **2009**, 2553–2555.
(79) Masci, G.; Giacomelli, L.; Crescenzi, V. *J. Polym. Sci., Part A: Polym. Chem.* **2005**, *43*, 4446–4454.
(80) Matyjaszewski, K.; Xia, J., *Handbook of Radical Polymerization*; Matyjaszewski, K., Davis, T. P., Eds.; John Wiley & Sons: Hoboken, NJ, 2002; Chapter 11, pp 523−628.
(81) Jung, H.-M.; Lee, K.-S.; Um, S *Int. J. Hydrogen Energy* **2008**, *33*, 2072–2086.
(82) Peckham, T. J.; Schmeisser, J.; Holdcroft, S. *J. Phys. Chem. B* **2008**, *112*, 2848–2858.
(83) Siu, A.; Schmeisser, J.; Holdcroft, S. *J. Phys. Chem. B* **2006**, *110*, 6072–6080.
(84) Cappadonia, M.; Erning, J. W.; Saberi Niaki, S. M.; Stimming, U. *Solid State Ionics* **1995**, *77*, 65–69.
(85) Anantaraman, A. V.; Gardner, C. L. *J. Electroanal. Chem.* **1996**, *414*, 115–120.

AM900690X